Available online at www.sciencedirect.com

SciVerse ScienceDirect

Ceramics International 38 (2012) 4517–4524

CERAMICS INTERNATIONAL

www.elsevier.com/locate/ceramint

Fracture toughness, strength and creep of transparent ceramics at high temperature

Marek Boniecki *, Zdzisław Librant, Anna Wajler, Władysław Wesołowski, Helena Węglarz

Institute of Electronic Materials Technology, 133 Wólczyńska Str, 01-919 Warsaw, Poland

Received 5 November 2011; received in revised form 3 February 2012; accepted 10 February 2012
Available online 7 March 2012

Abstract

Fracture toughness, four-point bending strength of transparent spinel, Y_2O_3 and YAG ceramics in function of temperature (from room temperature up to 1500° C) were measured. Creep resistance at 1500–1550° C was studied too. Grain size distribution was determined on polished and etched surfaces of samples. Fracture surfaces after tests were examined by scanning electron microscopy. The obtained results showed that: in the case of spinel ceramics fracture toughness and strength decreased from 20 to 800° C, increased from 800 to 1200° C and decreased at higher temperature; in the case of Y_2O_3 ceramics they increased from 400 to 800° C, and next kept constant up to 1500° C; in the case of YAG ceramics they kept constant from 20 to 1200° C and then decreased. The creep strain rate was measured for spinel and YAG but not for Y_2O_3 ceramics which appeared creep resistant. The hypotheses concerning toughening and creep mechanisms were proposed.

Keywords: C. Creep; C. Fracture; C. Strength; Transparent ceramics

1. Introduction

Transparent ceramics have recently acquired a high degree of interest. The basic applications are high-energy lasers, transparent armour windows, nose cones for heat seeking missiles, space exploration, security and medical imaging application. Most important application of transparent ceramics in the near future will probably be using them for the high-power solid state laser construction. For such application materials must have good thermal conductivity and thermal shock resistance, be scalable to large aperture sizes and be capable of being designed to produce a good quality beam. Transparent ceramics can uniquely provide these properties.

Transparency of polycrystalline material such as monophase ceramics is a result of specific state of materials microstructure. Ceramics produced by means of traditional technology contains several structural defects such as residual pores, inclusions and secondary phases, which scatter incident beam of light so that material is to some extent translucent if not opaque. Elimination of these structural defects is possible by using very pure (better than 4 N) nanometric oxide powder and by using pressure-assisted methods of sintering like hot pressing or hot isostatic pressing (HIP) or vacuum sintering, etc. When pores and other imperfections are nearly removed, sintered materials become transparent.

Such transparent ceramics with optical qualities comparable to those of single crystals of similar compositions have been developed in recent years [1]. As stated above, this is a result of improvement of fabrication technology of these ceramics mainly by a significant progress in pure powder preparation and in sintering methods. These high-temperature materials with good thermal and mechanical properties can replace traditionally used materials as glass and quartz in some armour applications or in lamp envelopes and infrared emitter and detector covers production. The most known and common ceramics as alumina (α-Al_2O_3) is rather translucent than transparent. It is birefringent as a results of its hexagonal structure. The birefringence leads to the light scattering in a polycrystalline material [2]. In order to avoid this disadvantageous phenomenon ceramics with cubic crystal lattice should be used. In Institute of Electronic Materials Technology cubic transparent ceramics as: spinel $MgAl_2O_4$, yttria Y_2O_3 and yttrium aluminium garnet, YAG ($Y_3Al_5O_{12}$), were prepared.

* Corresponding author.
E-mail addresses: Marek.Boniecki@itme.edu.pl, Marek-Boniecki@wp.pl (M. Boniecki).

0272-8842/$36.00
doi:10.1016/j.ceramint.2012.02.028

Nomenclature

A	dimensionless constant in creep equation
b	Burger vector
B	sample width
c_k	notch length
d	grain size
D	diffusion coefficient
D_l	lattice diffusion coefficient
G	shear modulus
k	Boltzmann's constant
K_{Ic}	fracture toughness
L and l	outer and inner span respectively
n	stress exponent in creep equation
p	grain size exponent in creep equation
P_c	breaking load
s	plastic zone extension
T	temperature
W	sample thickness
Y	geometric factor
$d\varepsilon/dt$	strain rate
σ	applied stress
σ_c	strength

For potential applications of these ceramics information about their mechanical properties is needed. So the purpose of the work is to obtain the data of the fracture toughness, bending strength and creep of the above mentioned transparent ceramics.

2. Literature review

In the case of spinel ceramics, given in [3,4] values of bending strength σ_c and of the fracture toughness K_{Ic} differ from each other. In addition, we observe a different character of changes of the fracture toughness as a function of temperature. For example, in [3] for temperatures above 900° C there was a decrease, while in [4] in the temperature range of 800–1200° C increase in K_{Ic}. It was shown in [5] that for Y_2O_3 ceramics samples the bending strength curiously increased above 600° C up to temperature of 1400° C from about 147 MPa to 210 MPa accordingly for the ceramics with grain size about 15 μm. However, for the ceramics with grain size about 0.7 μm the bending strength was independent of temperature from 20 to 1200° C (it equalled about 220 MPa) then decreased. In the case of YAG ceramics values of bending strength in the temperature range of 1100–1250° C [6] did not change as a function of temperature for 1 mm/min strain rate, but decreased for the strain rate 0.0016 mm/min above 1150° C, which was interpreted as the appearance of deformation plastic. In turn the fracture toughness K_{Ic} for YAG remains constant in the temperature range of 20–800° C, and next a slight increase in the temperature range of 800–1000° C and decreased in the range of 1000–1200° C [7] is observed. Spinel ceramics (average grain size about 1.3 μm) was deformed in superplastic way at 1450–1550° C with strain rate from 8.3×10^{-5} to $3.3 \times 10^{-3}\ s^{-1}$ [8]. It was shown in [9] that high purity polycrystalline yttria (the mean grain size about 0.6 μm) exhibits a high ductility, with elongation over 40%, for temperatures between 1400 and 1550° C, with strain rate from $10^{-3}\ s^{-1}$ to $10^{-4}\ s^{-1}$. Creep at rates from $10^{-5}\ s^{-1}$ to $10^{-3}\ s^{-1}$ was observed for samples of YAG ceramics with grain size of about 3 μm in the range of temperatures from 1400 to 1610° C [10].

The literature review suggests that given in the literature data on these properties of the ceramics are fragmentary and sometimes contradictory, depending on the preparation of samples and the methods of measurement. It creates a need of additional study making in order to obtain more complete and precise data concerning these properties of transparent ceramics.

3. Experimental procedure

3.1. Sample preparations

In order to obtain transparent spinel and yttria samples hot pressing with 1 wt.% of LiF was applied. The following powders were used: $MgAl_2O_4$ powder S30CR supplied by Baikalox (99.95% pure), Y_2O_3 powder supplied by Metall Rare Earth (99.999% pure) and LiF powder (99.995% pure, Aldrich). In both cases step-wise addition of uniaxial pressure was applied up to the maximum value of 30 MPa. Spinel and yttria samples were sintered in argon for 2 h at 1550° C and 1450° C, respectively.

The YAG ceramic plates of nominal 2 at.%. Nd dopant were produced by a solid-state reaction of high-purity (4 N) nanometric oxides powders i.e. Al_2O_3, Y_2O_3 and Nd_2O_3. Two commercially available oxides were applied, namely alumina powder of Taimei TM-DAR 4836, having mean crystallite size about 190 nm and specific area of 13.2 m^2/g and high-purity (5 N) neodymium oxide powder of Auer Remy with 40 nm mean crystallite size. Yttrium oxide nanopowder (XRD crystallite size of 79 nm) was produced by precipitation from water solution of high-purity hydrated nitrate, by means of ammonia hydrocarbonate. Aluminum, yttrium and neodymium oxides with addition of 0.5 mass% of tetraethyl orthosilicate (TEOS), were mixed by attrition milling and granulated. Granulated powder was uniaxially densified by cold isostatic pressing at 120 MPa in order to obtain plates, which next were sintered in Balzers MOV-3 vacuum (1.3×10^{-3} Pa) furnace at 1750° C for 6 h. After cutting and grinding of sintered plates bars of 2.5 mm × 4 mm × 30 mm and 1 mm × 4 mm × 30 mm were obtained.

3.2. Mechanical tests

Mechanical characterization of the ceramics, from room temperature up to 1550° C was made using universal testing machine Zwick 1446 equipped with a furnace.

In order to determine the material properties such as a bending strength σ_c and a fracture toughness K_{Ic}, the samples

were made in the shape of rectangular bars with dimensions of 2.5 mm × 4 mm × 30 mm. Strength measurements were carried out in four-point bending system at a distance of the lower support $L = 20$ mm and the upper $l = 10$ mm and for a loading rate 1 mm/min. Strength was calculated from (1):

$$\sigma_c = \frac{1.5P_c(L-l)}{BW^2} \quad (1)$$

where P_c is a breaking load, B is the sample width = 4 mm and W is the sample thickness = 2.5 mm.

Measurements of fracture toughness K_{Ic} were performed in three-point bending system with support distance $L = 20$ mm for bars with notches and for a loading rate of 1 mm/min. Notches were incised in the middle of the samples along the height using a circular saw with a width of 0.2 mm to a depth of about 0.9 mm and next to a final depth $c_k = 1.1$ mm using saw with a width of a 0.025 mm. K_{Ic} was calculated from (2):

$$K_{Ic} = Y\frac{1.5P_cL}{BW^2}c_k^{0.5} \quad (2)$$

where Y is a geometric constant calculated according to [11], $B = 2.5$ mm, $W = 4$ mm.

Creep resistance measurements were carried out in four-point bending system on the beams of dimensions 1 mm × 4 mm × 30 mm. The measurements were carried out at constant load registering a change of deformation. The rate of creep as a function of the applied stress was determined on the basis of procedure given in [12].

3.3. Microstructure studies

In order to obtain microscope pictures of microstructures some of the polished samples were etched in order to reveal the microstructure. Spinel and YAG samples were thermally etched accordingly at 1450° C for 1 h and at 1700° C for 6 h in air but Y_2O_3 samples were chemically etched in boiling water solution of HCl for 3 min. Next, the microstructure seen under the optical microscope (Zeiss) was analyzed with the computer programme for Feret's diameter method in order to obtain grain size distribution.

Fracture surfaces after K_{Ic} tests (in particular the area around the forehead incisions) were examined in the scanning electron microscope Opton DSM-950.

4. Results and discussion

Microstructure of the tested materials with grain size d are shown in Fig. 1. In Fig. 2 the dependence on temperature of four-point bending strength σ_c and fracture toughness K_{Ic} is shown for the studied ceramics. The mean values and standard deviations shown in the diagrams for each data point were calculated for five samples. The validity of the obtained results of K_{Ic} using a method which has been termed single edge notch bend – saw cut (SENB-S) needs some comments. The major limiting feature of SENB-S method is the appearance of a critical notch root radius ρ_c [13], above which the values of K_{Ic} are too high. It means that the values of K_{Ic} are valid if the notch thickness is below ρ_c. The magnitude of ρ_c is proportional to the size of the critical fracture-initiating defect in front of the notch. The size of this defect correlates, in turn, with some microstructural features especially with grain size. It was shown in [13] that for instance for alumina ceramics with mean grain size about 10 μm ρ_c was about 30 μm. In our case the smallest grain size (for YAG) is about 11 μm. It means that in our case ρ_c probably equals 30 μm too. In order to attain the final depth of the notch we used the saw with a width of 25 μm so the condition that notch thickness is below ρ_c seems to be satisfied and hence the obtained results of K_{Ic} are believed to be close to the true value.

In order to reveal the mode of fracture as a function of temperature, the fracture surfaces near crack tip of notched samples were observed by scanning electron microscopy (Fig. 3).

An unexpected feature is observed in Fig. 2 for spinel: σ_c decreases as a function of temperature up to 800° C and increased up to 1200° C. The low-temperature ($T < 800$° C) decreasing K_{Ic} region is attributed to the decrease in the elastic modulus with temperature [4]. In turn, the increase of K_{Ic} at higher temperatures could be connected with the appearance of crack tip plasticity at elevated temperature [4]. In this situation, the following relationship proposed in [14] between σ_c and plastic zone extension s at the crack tip can be applied:

$$\sigma_c = \sigma_{c0}\sqrt{\frac{2s}{2s+d}} \quad (3)$$

where $\sigma_{c0} = 111$ MPa is the strength of spinel at room temperature, $d = 21$ μm is a median grain size of spinel.

It was evaluated from Eq. (3) that for $\sigma_c = 66$ MPa at 800° C, $s \approx 6$ μm, but for $\sigma_c = 95$ MPa at 1200° C, $s \approx 29$ μm. It means that the plastic zone increases as a function of temperature which seems to be obvious. A similar effect as for σ_c is observed for K_{Ic}. The increase of K_{Ic} for spinel at temperatures higher than 800° C is also registered in [4] This phenomenon was explained by plasticity of crack tip due to cation diffusion [4]. The micrographs analyses of fracture surfaces (Fig. 3), made by scanning electron microscope, indicate that there is a mixed transgranular and intergranular mode of fracture but it seems that at high temperatures prevails rather intergranular one. The increased fraction of intergranular fracture and probably arising of plastic zone ahead of crack tip can cause the increase of σ_c and K_{Ic} at temperatures higher than 800° C for spinel.

For Y_2O_3, one can see a significant increase of K_{Ic} and σ_c between 400 and 800° C and slight fluctuations in the values of them in the range of 800–1500° C (Fig. 2). The effect of σ_c increase above 600° C up to temperature of 1400° C was observed in [5] for the average grain size of the ceramics about 15 μm, but for grain size about 0.7 μm σ_c was independent on temperature from 20 to 1200° C, then decreased. Photos of fracture surfaces of Y_2O_3 ceramics (Fig. 3) show that at room temperature fractures are transgranular, but at $T = 1500$° C fractures have mixed character (trans and intergranular). Probably a change of the fracture character is the result of intergranular boundaries weakness in the high-temperature

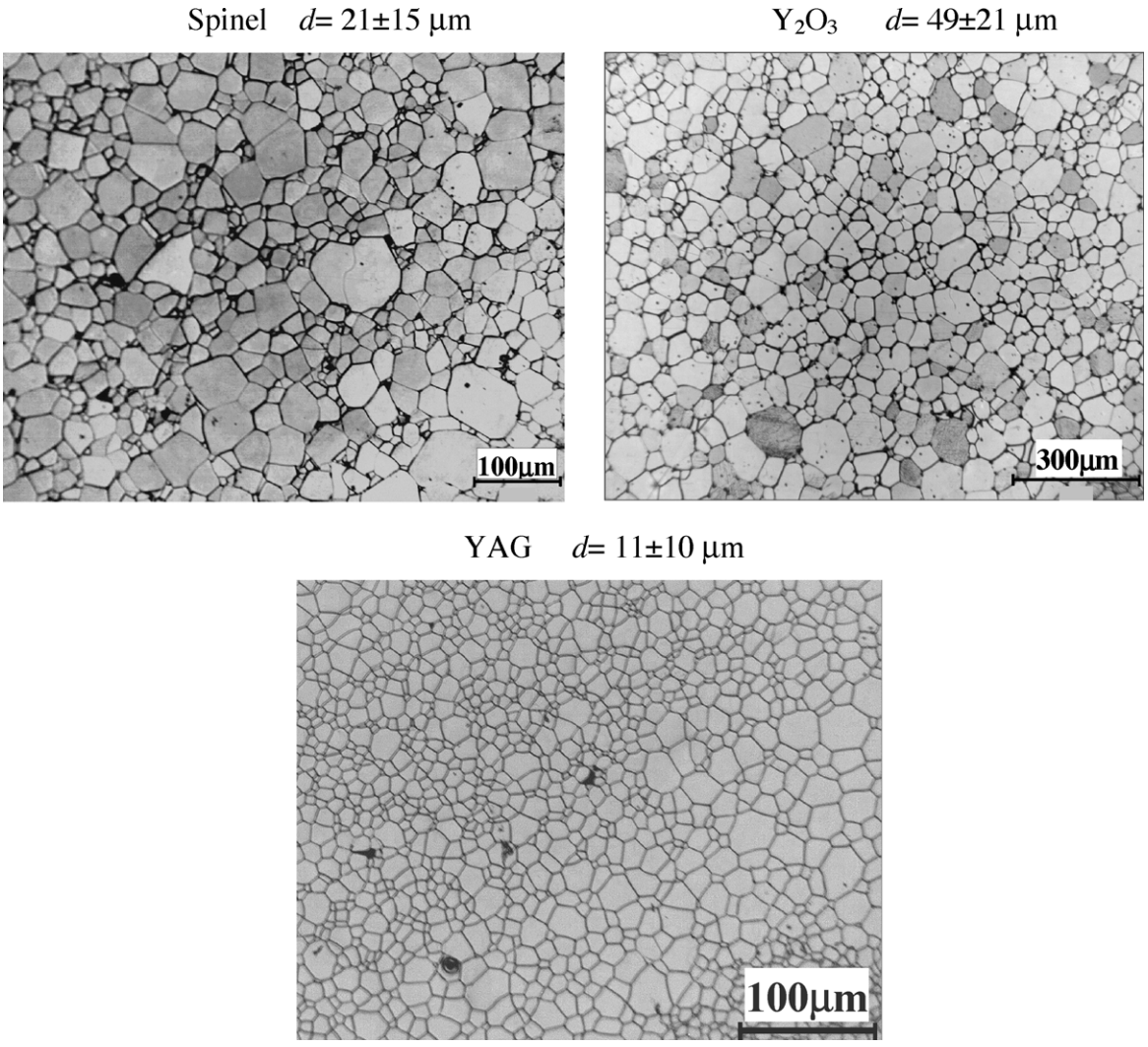

Fig. 1. Optical micrographs of polished and etched surfaces of the ceramics used in mechanical tests.

which means that cracks prefer to propagate intergranularly, which causes their deflection and next leads to the greater fracture toughness of the material [15].

For the YAG in the temperature range from 20 to 1200° C only a slight variation of σ_c and K_{Ic} is observed; above 1200° C they significantly decrease (Fig. 2). These results are consistent with data presented in [6,7]. Observations of YAG fracture surfaces suggest that cracking of samples proceeded mainly in the grain boundaries in the entire temperature range. No suggestions concerning fracture mechanics of YAG have been found.

Relationships between strain rate $d\varepsilon/dt$ and applied stress σ and temperature T are given in Fig. 4 for spinel and YAG ceramics. There was no measurable deflection of Y_2O_3 samples after loading for 2 h under a stress of 60 MPa at a temperature of 1550° C (the maximum attainable in the furnace placed on the testing machine). Increasing of stress resulted in breaking of the samples.

Creep is defined as a process of slow, continuous plastic deformation, which occurs at a stress below the yield point. Creep strain rate is described by (4) [16,17]:

$$\frac{d\varepsilon}{dt} = \frac{ADGb}{kT}\left(\frac{b}{d}\right)^p\left(\frac{\sigma}{G}\right)^n \quad (4)$$

where A is dimensionless constant, D is the appropriate diffusion coefficient = $D_0 \exp(-Q/RT)$ (where D_0 is a frequency factor, Q is the activation energy, R is the gas constant), G is shear modulus, b is Burger vector, p is the grain size exponent, n is stress exponent, k is the Boltzmann's constant, the rest of parameters were defined earlier.

The stress exponent n calculated as a slope of graphs in $\log(d\varepsilon/dt)$ vs $\log(\sigma)$ coordinates in Fig. 4 equals: 1.4, 2.0 for spinel and 2.1, 2.9 for YAG at 1500 and 1550° C respectively. In turn activation energy Q calculated as a slope of graphs in $\log(d\varepsilon/dt)$ vs $\log(1/T)$ coordinates equals accordingly (for σ = 40 MPa) 672 and 904 kJ/mol for spinel and YAG ceramics. In comparison in [8] for spinel with average grain size about 1.3 μm deformed in the range of T 1450–1550° C, $n = 1.8 \pm 0.3$ but $Q = 500 \pm 50$ kJ/mol then they are consistent

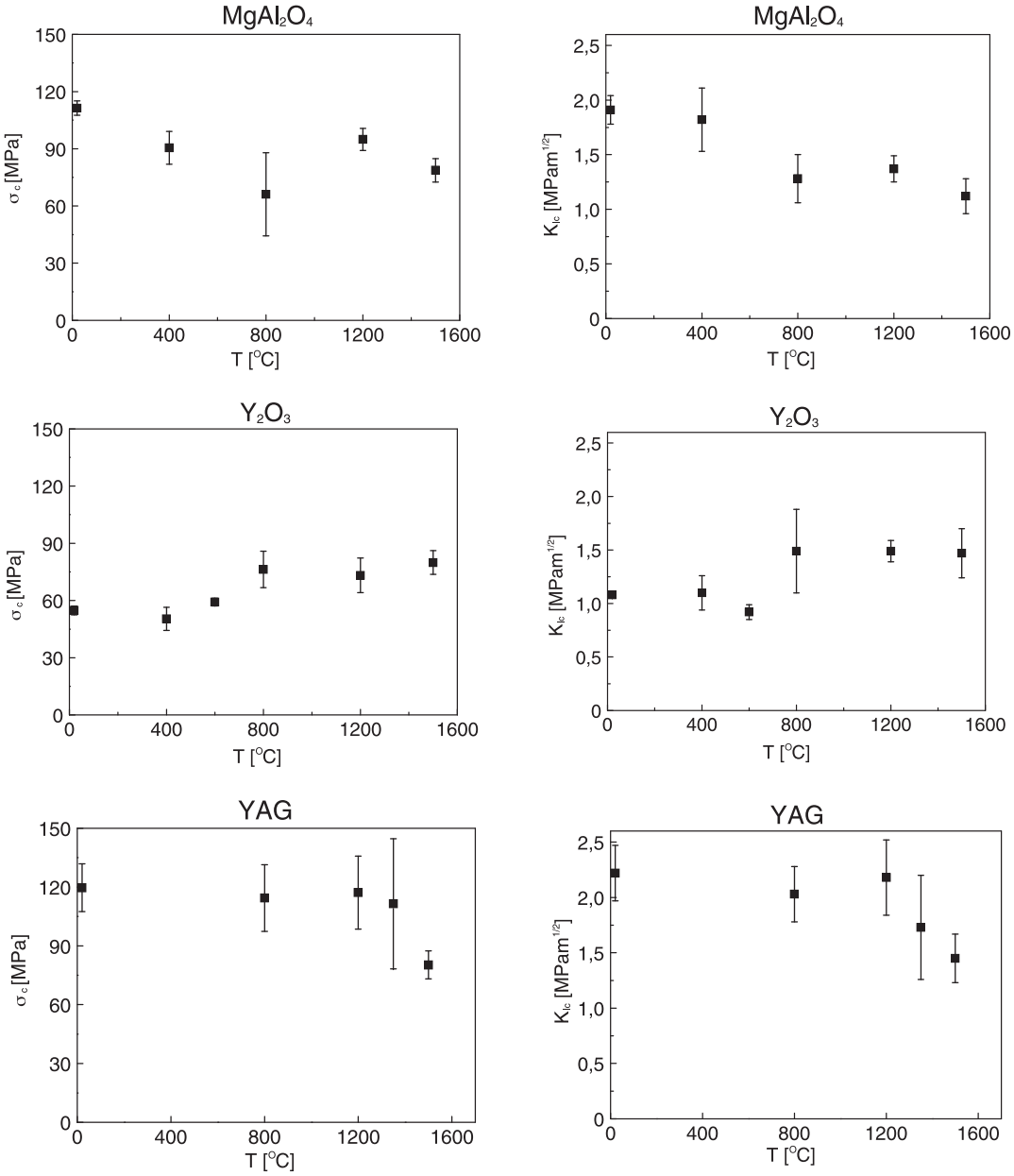

Fig. 2. Fracture toughness K_{Ic} and bending strength σ_c vs temperature T for the studied ceramics.

with our results. However data given for YAG ($d = 3$ μm) in [10] $n = 1.24 \pm 0.1$ and $Q = 584 \pm 26$ kJ/mol (obtained at the temperature range of 1400–1610° C) differ significantly from our results. According to [8] one can claim that creep deformation in spinel occurs with the participation of grain boundary sliding with strain rate controlled by the dislocation recovery limited by the lattice diffusion of oxygen ions. In turn for YAG ceramics it is suggested [10] that creep obeys the Nabarro–Herring model [16,17] with bulk diffusion of one of the cations as strain rate limiting. On the base on creep theory some equations were proposed [16,17] in which parameters shown in Eq. (4) are defined. For instance, for spinel creep results interpretation Nabarro Eq. (5) seems to be suitable. Nabarro equation was derived assuming that strain rate of creep is controlled by the climb of edge dislocations. In turn, the rate of climb of the dislocations is determined by the diffusion of atoms or ions, which oscillate with the thresholds for dislocation line to the holes in the immediate vicinity of dislocation lines or attach themselves to these thresholds, resulting in the holes in the environment.

$$\frac{d\varepsilon}{dt} = \frac{0.22 D_l G b}{kT} \left(\frac{\sigma}{G}\right)^3 \tag{5}$$

where D_l is a lattice diffusion coefficient, the rest of the parameters were defined earlier.

In turn Nabarro–Herring Eq. (6) [16,17] seems to be suitable for YAG creep explanation. It was derived assuming that strain

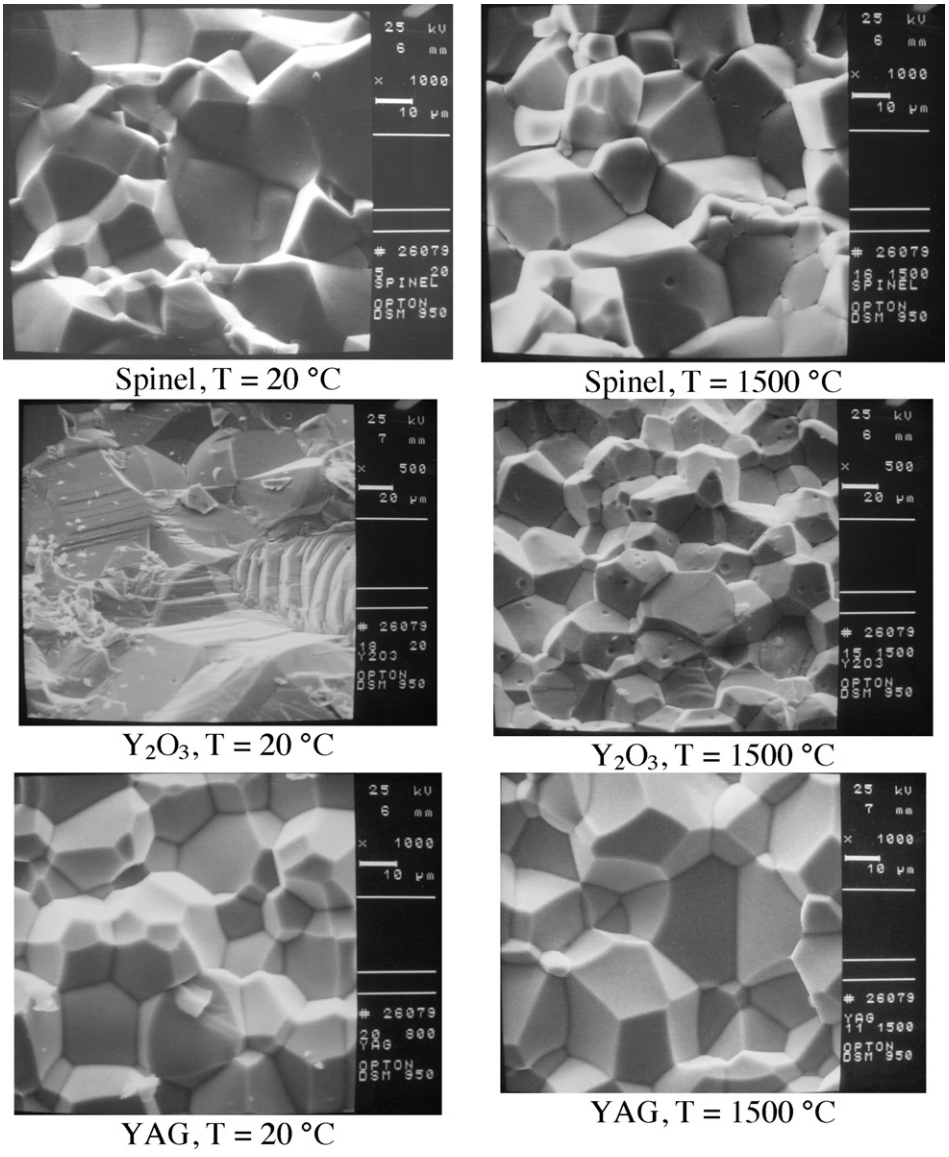

Fig. 3. Scanning electron micrographs of fracture surfaces of studied ceramics at room and at the highest temperature.

rate of creep is controlled by vacancy flow through the lattice.

$$\frac{d\varepsilon}{dt} = \frac{9.3 D_l b}{kT}\left(\frac{b}{d}\right)^2 \sigma \tag{6}$$

Additionally, in [10] the experimental equation for YAG ceramics creep was derived.

$$\frac{d\varepsilon}{dt} = \frac{4.52 \times 10^{-21}}{kTd^2}\exp\left(-\frac{584\,\mathrm{kJ/mol}}{RT}\right)\sigma^{1.24} \tag{7}$$

In Fig. 5 a comparison of the creep strain rate $d\varepsilon/dt$ for spinel and YAG ceramics calculated from Nabarro, Nabarro–Herring [16,17] and Parthasarathy et al. [10] equations (presented in the form of lines) with experimental results (presented in the form ■) at $T = 1550^\circ$ C was made. In the calculations of $d\varepsilon/dt$ for spinel it was assumed that Burgers vector $b = 0.57$ nm [8], lattice diffusion coefficient $D_l = D_O$ (at $T = 1550^\circ$ C) $= 2.2 \times 10^{-17}$ m^2/s [18] (D_O is a lattice diffusion of oxygen ions), shear modulus $G = 89.2$ GPa [4] at 1550° C and $d = 21$ μm.

In the calculations of $d\varepsilon/dt$ for YAG it was assumed that Burgers vector $b = 1.04$ nm [19], lattice diffusion coefficient $D_l = D_Y$ (at $T = 1550^\circ$ C) $= 5.5 \times 10^{-18}$ m^2/s [19] (D_Y is a lattice diffusion of yttrium ions), shear modulus $G = 90$ GPa at 1550° C [19] and $d = 11$ μm.

As shown in Fig. 5 according to the assumptions put forward earlier $d\varepsilon/dt$ the values for spinel calculated by the formula Nabarro are much closer to experimental results than those calculated by Nabarro–Herring formula. In turn for YAG the obtained experimental results are within the range of values assigned to Eq. (6) (Nabarro–Herring'a) and Eq. (7) (Parthasarathy et al.) for the assumption that yttrium ion lattice diffusion is responsible for the creep in this ceramics.

The lack of the creep results for yttria needs some comments. In [9] it was suggested that diffusion of yttrium ions plays the main role in yttria creep. Assuming that creep

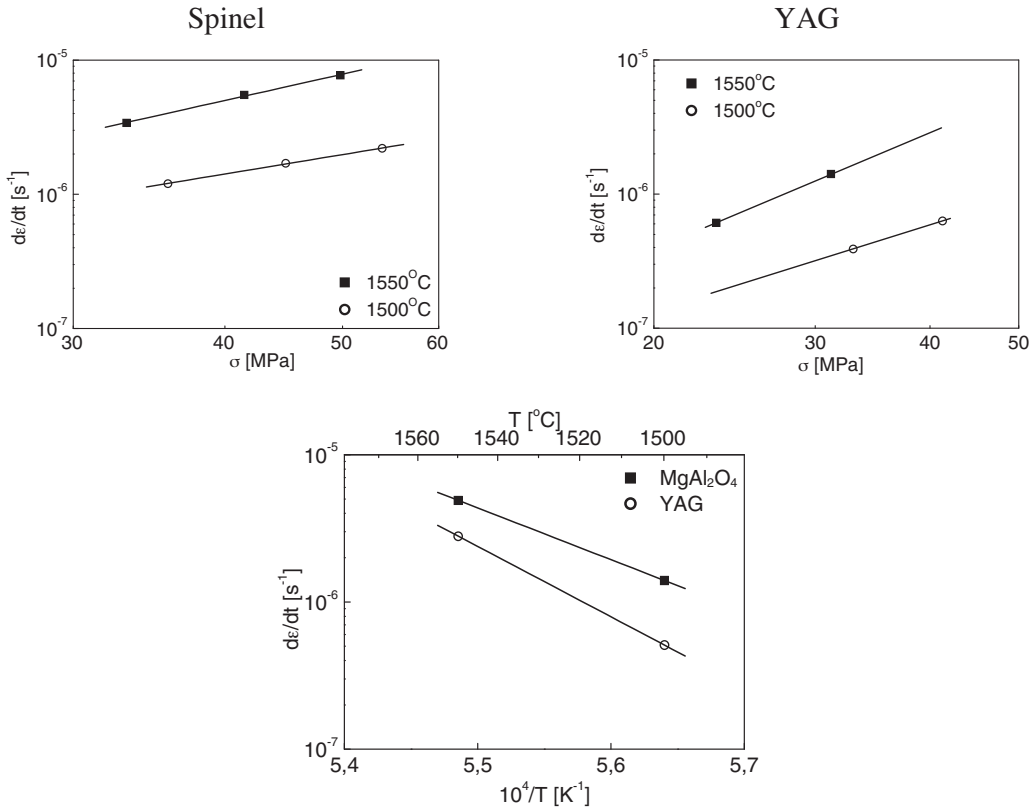

Fig. 4. Strain rate $d\varepsilon/dt$ as a function of stress σ and temperature T for spinel and YAG ceramics. Temperature dependence is shown for $d\varepsilon/dt$ taken for $\sigma = 40$ MPa.

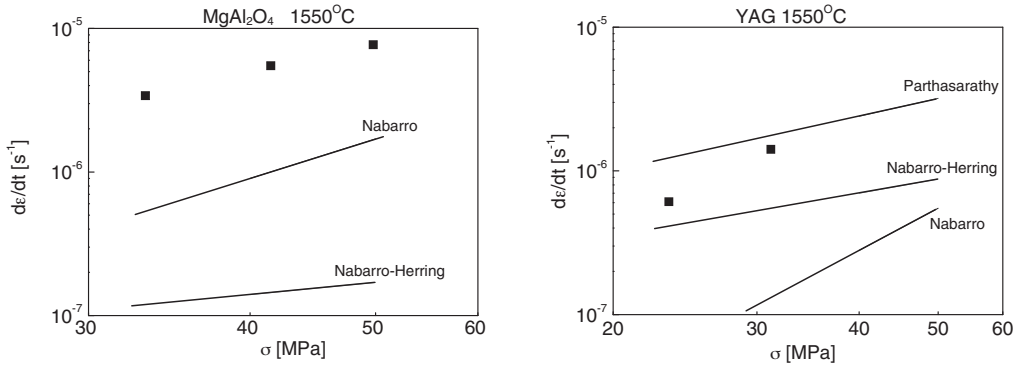

Fig. 5. Comparison of the creep strain rate $d\varepsilon/dt$ for spinel and YAG ceramics calculated from Eqs. (5)–(7) (presented in the form of lines) with experimental results (presented in the form ■) at $T = 1550^\circ$ C.

could be described by Nabarro–Herring Eq. (6) one can see that $d\varepsilon/dt \sim D_Y/d^2$. For YAG and yttria (at 1550° C) $D_Y = 5.5 \times 10^{-18}$ m^2/s and 7.9×10^{-18} m^2/s [19,20] respectively but $d = 11$ and 49 μm respectively. Hence $\dot{\varepsilon}_{Y_2O_3}/\dot{\varepsilon}_{YAG} \approx 1/14$ and strain rate for yttria is smaller than 10^{-7} s^{-1}. It is too small for registration in our measurement system.

5. Conclusion

In this work selected mechanical properties as a function of temperature for three transparent ceramics: spinel ($MgAl_2O_4$), yttria (Y_2O_3), and YAG ($Y_3Al_5O_{12}$) were investigated. For all the ceramics bending strength σ_c and fracture toughness K_{Ic} behave in another way in function of temperature: in the case of spinel σ_c and K_{Ic} decreased from 20 to 800° C, increased from 800 to 1200° C and decreased at higher temperature; in the case of yttria they increased from 400 to 800° C, and next kept constant up to 1500° C; in the case of YAG they kept constant from 20 to 1200° C and then decreased. Yttria appeared the most creep resistant ceramics but spinel the least creep resistant. Creep mechanisms for spinel and YAG were proposed on the base of the literature reports.

Acknowledgement

This work was supported by the Polish Ministry of Education and Science (Project No. 438/E-241/S/2010).

References

[1] A. Krell, T. Hutzler, J. Klimke, Transmission physics and consequences for materials selection, manufacturing and applications, J. Eur. Ceram. Soc. 29 (2009) 207–221.

[2] R. Apetz, M.P.B. van Bruggen, Transparent alumina: a light-scattering model, J. Am. Ceram. Soc. 86 (2003) 480–486.

[3] R.L. Stewart, R.C. Bradt, Fracture of polycrystalline $MgAl_2O_4$, J. Am. Ceram. Soc. 63 (1980) 619–623.

[4] C. Baudin, R. Martinez, P. Pena, High-temperature mechanical behavior of stoichiometric magnesium spinel, J. Am. Ceram. Soc. 78 (1995) 1857–1862.

[5] M. Desmaison-Brut, J. Montintin, E. Valin, M. Boncoeur, Influence of processing conditions on the microstructure and mechanical properties of sintered yttrium oxide, J. Am. Ceram. Soc. 78 (1995) 716–722.

[6] H. Nozawa, T. Yanagitani, T. Nishimura, H. Tanaka, Mechanical properties of fully dense yttrium aluminum garnet (YAG) ceramics, J. Ceram. Soc. Jpn. 116 (2008) 649–652.

[7] J.D. French, H.M. Chan, M.P. Harmer, G.A. Miller, High-temperature fracture toughness of duplex microstructures, J. Am. Ceram. Soc. 79 (1996) 58–64.

[8] K. Morita, K. Hiraga, B.N. Kim, T.S. Suzuki, Y. Sakka, Strain softening and hardening during superplastic-like flow in a fine-grained $MgAl_2O_4$ spinel polycrystal, J. Am. Ceram. Soc. 87 (2004) 1102–1109.

[9] T. Rouxel, D. Murat, J.L. Besson, M. Boncoeur, Large tensile ductility of high purity polycrystalline yttria, Acta Mater. 44 (1996) 263–278.

[10] A.T. Parthasarathy, T.I. Mach, K. Keller, Creep mechanism of polycrystalline yttrium aluminum garnet, J. Am. Ceram. Soc. 75 (1992) 1756–1759.

[11] T. Fett, D. Munz, Subcritical crack growth of macrocracks in alumina with R-curve behavior, J. Am. Ceram. Soc. 75 (1992) 958–963.

[12] G.W. Hollenberg, G.R. Terwilliger, R.S. Gordon, Calculation of stresses and strains in four-point bending creep tests, J. Am. Ceram. Soc. 54 (1971) 196–199.

[13] R. Damani, R. Gstrein, R. Danzer, Critical notch-root radius effect in SENB-S fracture toughness testing, J. Eur. Ceram. Soc. 16 (1996) 695–702.

[14] R.W. Armstrong, Grain size dependent alumina fracture mechanics stress intensity, Int. J. Refract. Met. Hard Mater. 19 (2001) 251–255.

[15] D.R. Clarke, K.T. Faber, Fracture of ceramics and glasses, J. Phys. Chem. Sol. 48 (1987) 1115–1157.

[16] R.G. Cannon, T.G. Langdon, Review Creep of ceramics. Part 2. An examination of flow mechanisms, J. Mater. Sci. 23 (1988) 1–20.

[17] A.H. Chokshi, T.G. Langdon, Characteristic of creep deformation in ceramics, Mater. Sci. Technol. 7 (1991) 577–584.

[18] K. Ando, Y. Oishi, Self-diffusion coefficients of oxygen ion in single crystals of $MgO{\cdot}nAl_2O_3$ spinels, J. Chem. Phys. 61 (1974) 625–629.

[19] M. Jimenez-Melendo, H. Haneda, Ytterbium cation diffusion in yttrium aluminum garnet (YAG) – implication for creep mechanisms, J. Am. Ceram. Soc. 84 (2001) 2356–2360.

[20] R.J. Gaboriaud, Self-diffusion of yttrium in monocrystalline yttrium oxide: Y_2O_3, J. Solid State Chem. 35 (1980) 252–261.